

# Supplemental Information for Gravitational Wave Sensors Based on Superconducting Transducers

Armen Gulian,<sup>1,2,\*</sup> Joe Foreman,<sup>3</sup> Vahan Nikoghosyan,<sup>1,4</sup> Louis Sica,<sup>1</sup> Pablo Abramian-Barco,<sup>5</sup> Jeff Tollaksen,<sup>1,2</sup> Gurgen Melkonyan,<sup>1</sup> Iris Mowgood,<sup>1</sup> Chris Burdette,<sup>1</sup> Rajendra Dulal,<sup>1,2</sup> Serafim Teknowijoyo,<sup>1,2</sup> Sara Chahid,<sup>1,2</sup> and Shmuel Nussinov<sup>1,6</sup>

<sup>1</sup>*Advanced Physics Laboratory, Institute for Quantum Studies,  
Chapman University, Burtonsville, MD 20866, USA*

<sup>2</sup>*Schmid College of Science and Technology, Chapman University, Orange, CA 92866, USA*

<sup>3</sup>*Independent Researcher, Alexandria, VA 22310, USA*

<sup>4</sup>*Institute for Physics Research, National Academy of Sciences, Ashtarak, 0203, Armenia*

<sup>5</sup>*CIEMAT, Madrid 28040, Spain*

<sup>6</sup>*School of Physics and Astronomy, Tel-Aviv University, Ramat-Aviv, 69978, Tel-Aviv, Israel*

## COMSOL MODELING

Here we will describe our modeling approach which yields the results shown in Fig. 7 of the main text. The superconductor is treated in the framework of time-dependent Ginzburg-Landau equations [1, 2], which choosing the gauge  $\varphi \equiv 0$ , we represent as:

$$\frac{\pi}{8T_c} \frac{\partial \Psi}{\partial t} - \frac{\pi D}{8T_c} (\nabla - 2i\mathbf{A})^2 \Psi - \left[ \frac{T_c - T}{T_c} - \frac{7\zeta(3)|\Psi|^2}{8(\pi T_c)^2} \right] \Psi = 0, \quad (\text{S.1})$$

for the wave function of the pairs,  $\Psi$ , and

$$\mathbf{j} = -\frac{\pi\sigma}{4T_c} |\Psi|^2 (2\mathbf{A} - \nabla\theta) - \sigma_n \dot{\mathbf{A}}, \quad (\text{S.2})$$

for the current density  $\mathbf{j}$ ,  $\varphi$  and  $\mathbf{A}$  are the scalar and the vector potentials. The remaining coefficients are described below. We use here the so-called gapless limit of TDGL equations (a more general case of description by finite gap TDGL equations is discussed in [3]). It is convenient to rewrite these equations in a dimensionless form:

$$\frac{\partial \psi}{\partial \tau} = -\left(\frac{i}{\kappa} \tilde{\nabla} + \tilde{\mathbf{A}}\right)^2 \psi + (1 - |\psi|^2) \psi, \quad (\text{S.3})$$

and

$$\tilde{\sigma} \frac{\partial \tilde{\mathbf{A}}}{\partial \tau} = -\tilde{\nabla} \times \tilde{\nabla} \times \tilde{\mathbf{A}} - |\psi|^2 \left( \tilde{\mathbf{A}} - \frac{1}{\kappa} \tilde{\nabla}\theta \right), \quad (\text{S.4})$$

where we denoted:  $\psi \equiv \Psi/\Psi_0$ , where  $\Psi_0 = \sqrt{8\pi^2 T_c (T_c - T)/[7\zeta(3)]}$ ;  $\tau = t/t_0$ , where  $t_0 = \pi/(8\eta T_c)$  and  $\eta = (T_c - T)/T_c$ ;  $\kappa \equiv \lambda_L/\xi$  is the Ginzburg-Landau parameter:  $\kappa < 1/\sqrt{2}$  for type-I superconductors and  $\kappa > 1/\sqrt{2}$  for type-II superconductors, the London

penetration depth is defined by  $1/\lambda_L^2 = 2\pi^2\sigma\Psi_0^2/T_c = 16\pi^4\sigma(T_c - T)/[7\zeta(3)]$ , the coherence length equals  $\xi \equiv \sqrt{\pi D/[8(T_c - T)]}$ ,  $\sigma$  is the conductivity and  $D$  is the diffusion coefficient of normal electrons in superconductors;  $\tilde{\mathbf{A}} \equiv 2\xi\mathbf{A}$ ,  $\tilde{\nabla} \equiv \lambda_L\nabla$ , and  $\tilde{\sigma} \equiv 4\pi\lambda_L\sigma/t_0$ . In transferring from (S.2) to (S.4) we used Maxwell's equation (in Gaussian units with  $c = 1$ ):  $\nabla \times \mathbf{B} = 4\pi\mathbf{j} = \nabla \times \nabla \times \mathbf{A}$ . When using below Eqs. (S.3) and (S.4), we will drop tildes.

Since  $\psi$  is a complex function, (S.3) consists of two equations for two scalars:  $|\psi|$  and  $\theta$ , or, alternatively, real and imaginary parts of  $\psi$ :

$$\psi = |\psi|e^{i\theta} = \psi_1 + i\psi_2 = \text{Re}\psi + i\text{Im}\psi. \quad (\text{S.5})$$

The latter is more convenient for solving these equations. Then the system of TDGL equations can be represented in the form:

$$\begin{aligned} \dot{\psi}_1 &= \frac{1}{\kappa^2} (\psi_{1.xx} + \psi_{1.yy} + \psi_{1.zz}) \\ &+ \frac{2}{\kappa} (A_1\psi_{2.x} + A_2\psi_{2.y} + A_3\psi_{2.z}) \\ &+ \frac{\psi_2}{\kappa} (A_{1.x} + A_{2.y} + A_{3.z}) \\ &- \psi_1 (A_1^2 + A_2^2 + A_3^2 - 1 + \psi_1^2 + \psi_2^2), \end{aligned} \quad (\text{S.6})$$

$$\begin{aligned} \dot{\psi}_2 &= \frac{1}{\kappa^2} (\psi_{2.xx} + \psi_{2.yy} + \psi_{2.zz}) \\ &- \frac{2}{\kappa} (A_1\psi_{1.x} + A_2\psi_{1.y} + A_3\psi_{1.z}) \\ &- \frac{\psi_1}{\kappa} (A_{1.x} + A_{2.y} + A_{3.z}) \\ &- \psi_2 (A_1^2 + A_2^2 + A_3^2 - 1 + \psi_1^2 + \psi_2^2), \end{aligned} \quad (\text{S.7})$$

$$\begin{aligned} \sigma \dot{A}_1 &= -\frac{1}{\kappa} (\psi_2\psi_{1.x} - \psi_1\psi_{2.x}) - (\psi_1^2 + \psi_2^2) A_1 \\ &+ A_{1.yy} - A_{2.xy} - A_{3.xz} + A_{1.zz}, \end{aligned} \quad (\text{S.8})$$

$$\begin{aligned} \sigma \dot{A}_2 &= -\frac{1}{\kappa} (\psi_2\psi_{1.y} - \psi_1\psi_{2.y}) - (\psi_1^2 + \psi_2^2) A_2 \\ &+ A_{2.xx} - A_{1.xy} - A_{3.yz} + A_{2.zz}, \end{aligned} \quad (\text{S.9})$$

\* Corresponding author: gulian@chapman.edu

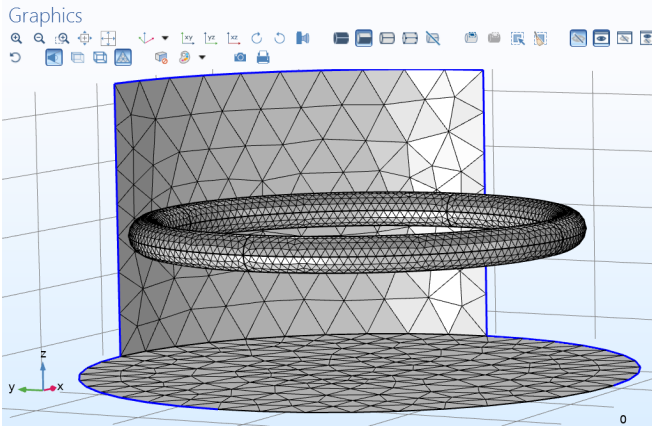


FIG. S1. Superconducting ring located in a cylindrical volume (top panel and some of side panels of the cylinder are removed for visibility). The Physics Controlled mesh with the Fine Element size used at modeling is shown.

$$\sigma \dot{A}_3 = -\frac{1}{\kappa} (\psi_2 \psi_{1,z} - \psi_1 \psi_{2,z}) - (\psi_1^2 + \psi_2^2) A_3 + A_{3,xx} - A_{1,xz} + A_{3yy} - A_{2,yz}. \quad (\text{S.10})$$

These equations are solved using the COMSOL modeling of the problem with the appropriate boundary and initial conditions to be specified below. In COMSOL, the Coefficient Form PDE system for  $\psi_1$  and  $\psi_2$ , and General Form PDE system for the components  $(A_1, A_2, A_3)$  of the vector potential were used.

We modeled the vertically stacked superconducting rings in a homogeneous vertically aligned magnetic field, which is switched on and off at given moments of time. We track the behavior of the currents in the rings for various ring numbers at a given distance between consecutive rings. Next we describe how this goal is achieved by the COMSOL code.

In the computation, the superconducting loop is regarded as a perfect torus, with the major radius  $r_0$  and minor radius  $r_1$ . This torus is placed inside of a cylinder with a radius  $R_0$  and a height  $Z_0$  (Fig. S1). These and other parameters used in the COMSOL code are listed in Fig. S2.

The magnetic field  $\mathbf{B}$  is described by the vector potential  $\mathbf{A}$ :  $\mathbf{B} = \nabla \times \mathbf{A}$ . In absence of superconducting rings we chose the  $\mathbf{A}$ -field of the form:

$$A_x = -B_{z0} \left( \Theta(t - t_0) \tanh[\omega_1(t - t_0)] - \Theta(t - t_1) \tanh[\omega_2(t - t_1)] \right) y/2 \quad (\text{S.11})$$

$$A_y = B_{z0} \left( \Theta(t - t_0) \tanh[\omega_1(t - t_0)] - \Theta(t - t_1) \tanh[\omega_2(t - t_1)] \right) x/2 \quad (\text{S.12})$$

$$A_z = 0 \quad (\text{S.13})$$

Parameters			
Name	Expression	Value	Description
R0	24	24	cylinder radius
Z0	24	24	cylinder height
r0	18	18	torus radius major
r1	1.5	1.5	torus radius minor
sigma	1	1	normal conductivity
sigmadiel	0.00000000001	1E-11	artificial conductivity
t0	2	2	field on begins
t1	10	10	field off begins
omega1	2	2	increase speed
omega2	1	1	decrease speed
t2	15	15	evolution time
Bz0	0.01	0.01	external magnetic field
kappa	0.4	0.4	G-L parameter

FIG. S2. The parameters used (and varied) for modeling the current excitation in a single loop. Here  $R_0$ , and  $Z_0$  describe the external cylinder which contains a homogeneous field with the amplitude  $H = B_{z0}$ . An artificial (and negligibly small) conductivity  $\sigma_{diel}$  is assigned to the internal cylinder volume – its role is discussed in the code description;  $\omega_1$  and  $\omega_2$  characterize the speed of the  $H$ -field increase and decrease correspondingly; the definition of the other parameters is indicated in the table.

to represent the homogeneous magnetic field along the  $z$ -axis. As is clear from the definition, the field is coming in and going out adiabatically, and, at modeling, both in- and out-speeds can be set via  $\omega$ -parameters. As we have found, the current amplitude does not depend anyhow essentially on these parameters (Fig. S3).

In the presence of the superconducting rings, the  $\mathbf{A}$ -field should be found as the solution of the system of equations (S.6)-(S.10). However, at sufficiently large distance (“infinity”) from the superconductor, the  $\mathbf{A}$ -field still should have the form (S.11)-(S.13), which then should be considered as the (Dirichlet) boundary conditions for it. In our model, the walls of the external cylinder represent the infinitely far boundary, so the Dirichlet boundary conditions (S.11)-(S.13) could be assigned to them. It is also very convenient to formulate the boundary conditions for the  $\Psi$ -function on these walls. In such a case, we should assume that equations (S.6) and (S.7) are valid not only inside the tori, but also inside the encompassing cylinder. The behavior of the superconducting tori in the magnetic field is the same when the tori and the magnetic field are in vacuum or when the tori are surrounded by non-magnetic non-conducting medium. The smallness of  $\sigma_{diel}$  guarantees that when the magnetic field is switched on and off, the current induced by Faraday’s law is negligible in this artificial surrounding substance where there are no Cooper pairs. For that to be the case, we introduce a function  $vol(x, y, z)$  which equals 1 inside of torus, and 0 outside of it. This function is defined as a *variable* in the COMSOL code, Fig. S4.

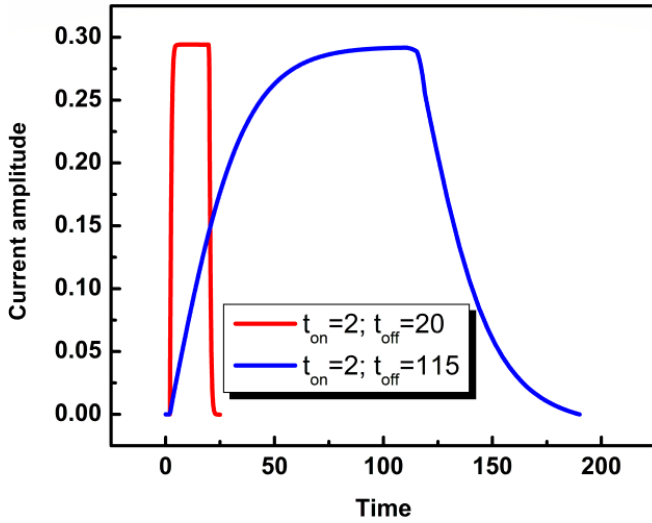


FIG. S3. The current amplitude does not depend on the speed of the external flux increase. These curves correspond to  $\omega_1 = \omega_2 = 1$  (red curve) and  $\omega_1 = \omega_2 = 0.03$  (blue curve). Others parameters are:  $R_0 = 40$ ,  $Z_0 = 20$ ,  $r_0 = 24$ ,  $r_1 = 2$ ,  $\kappa = 0.4$ ,  $B_{z0} = 0.01$ ,  $\sigma = 0.5$ . Dimensionless unit of time corresponds to  $\sim 10$  ps. Independence of the current amplitude on the speed of the flux variation is important since the dimensionless time unit at the modeling is much shorter than the characteristic GW time scale.

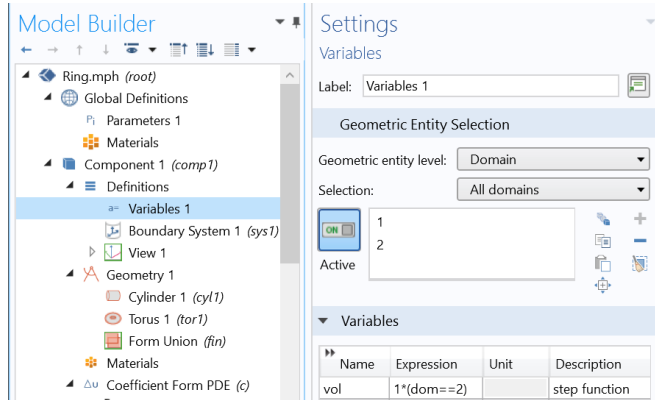


FIG. S4. Defining the *vol*-variable in COMSOL code. Domain 1 corresponds to the volume of cylinder, and domain 2 to the volume of torus. In the Boolean expression  $vol = 1$  in domain 2 and zero otherwise.

Multiplying of all the r.h.s.  $\Psi$ -terms in equations (S.6)-(S.10) by the variable *vol* will guarantee the vanishing of  $\Psi$  outside of the tori. One should also properly define the function  $\sigma$  which enters (S.8)-(S.10). Since these equations are valid in the COMSOL code for both the tori and the cylinder domains, we should have its value reduced to zero in the latter domain by redefining  $\sigma \rightarrow \sigma * vol + \sigma_{diel}$ , where the negligibly small quantity  $\sigma_{diel}$  is added to avoid division by zero at computer operations (as usual, one should confirm the convergence of the solutions as this artificial  $\sigma_{diel}$  is reduced to zero). To finalize the code

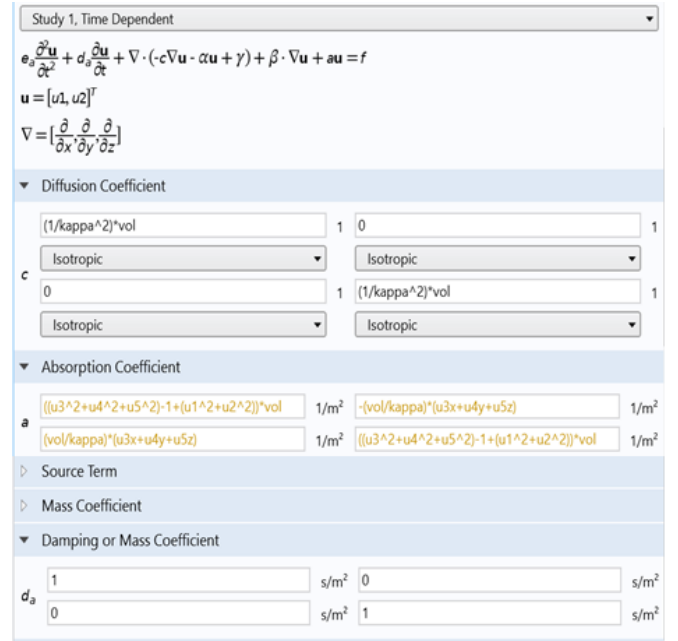


FIG. S5. COMSOL code for equations (S.6) and (S.7) within Coefficient Form PDE. The functions  $\Psi_1$  and  $\Psi_2$  correspond to  $u_1$  and  $u_2$ .



FIG. S6. COMSOL code for equations (S.8)-(S.10) within General Form PDE. The functions  $A_x$ ,  $A_y$  and  $A_z$  correspond to  $u_3$ ,  $u_4$  and  $u_5$ .

description we notice that now the formal mathematical formulation of the problem may be accomplished by assigning Dirichlet boundary conditions  $\psi_1 = \psi_2 = 0$  on the walls of the cylinder. The implementation of the differential equations (S.6)-(S.10) within COMSOL is sketched in Figs. S5 and S6.

The result shown in Fig. 7 of the main text, *top* panel, is plotted via 3D Plot Group of COMSOL, as the Surface plot for the Cooper-pair density  $u_1^2 + u_2^2$ , and two arrow volume plots for the current density  $\mathbf{j} = (j_x, j_y, j_z)$ , with  $j_x = vol * (u_{4xy} - u_{3yy} + u_{5xz} - u_{3zz})$ ,  $j_y = vol * (-u_{4xx} + u_{3xy} + u_{5yz} - u_{4zz})$ , and  $j_z = vol * (-u_{5xx} + u_{3xz} - u_{5yy} + u_{4yz})$  (green arrows) and the magnetic field  $\mathbf{B} = (B_x, B_y, B_z)$  with  $B_x = u_{5y} - u_{4z}$ ,  $B_y = -u_{5y} + u_{3z}$  and

$B_z = u_{4x} - u_{3y}$  (red arrows). The indices after variable names indicate partial derivatives. Color coding in this figure corresponds to the normalized density of Cooper pairs: it is maximal on the torus and zero on the walls of the cylinder. For multiple rings, no essential changes to the code should be done, only the cylinder height should be increased to continue serving as the infinitely large volume, and the variable *vol* (Fig. S4) should be redefined so as to include all the rings domains.

To obtain the current and the flux from these computational data one needs just to cross the ring (or rings) by appropriate planes and perform the required integrations – this is achieved via standard COMSOL procedures.

- 
- [1] A. Gulian, *Shortcut to Superconductivity: Superconducting Electronics via COMSOL Modeling* (Springer International Publishing, 2020).
- [2] L. P. Gor'kov and G. M. Éliashberg, *Generalization of the Ginzburg-Landau Equations for Non-stationary Problems in the Case of Alloys with Paramagnetic Impurities*, Soviet

- Journal of Experimental and Theoretical Physics **27**, 328 (1968), [Zh. Eksp. i Teor. Fiz. **54**, 2 612 (1968)].
- [3] I. Mowgood, G. Melkonyan, R. Dulal, S. Teknowijoyo, S. Chahid, and A. Gulian, Violation of magnetic flux conservation by superconducting nanorings, Superconductor Science and Technology (submitted).